Choosing a suitable analytical model for aerosol extinction spectra in the retrieval of UV/visible satellite occultation measurements

F. Vanhellemont,[1] D. Fussen,[1] J. Dodion,[1] C. Bingen,[1] and N. Mateshvili[1]

Received 1 December 2005; revised 3 August 2006; accepted 17 August 2006; published 6 December 2006.

[1] In the retrieval of satellite occultation experiments the optical extinction by atmospheric gases can be adequately modeled as the product of an extinction cross section with the number density. For aerosols the situation is more complex. Usually, the extinction spectrum is modeled by some analytical function of wavelength, controlled by a small number of parameters. However, a consensus about which function to use does not exist. The goal of this paper is to find out which analytical function is most suitable and how many parameters are necessary to capture the background aerosol extinction behavior. To do this, we first retrieve atmospheric constituent altitude profiles from a set of simulated spectra, measured by a virtual instrument of which the characteristics are based on the ones from the Global Ozone Monitoring by Occultation of Stars (GOMOS) instrument. Several aerosol extinction models are used in the retrieval. The effect of the aerosol model choice on the retrieval error and bias is then calculated by comparing the retrieved profiles with the ones that were used in the simulation. The results show that the use of a second-degree polynomial leads to good retrievals of aerosol extinction coefficients, while simpler models already give very acceptable results for the other species.

Citation: Vanhellemont, F., D. Fussen, J. Dodion, C. Bingen, and N. Mateshvili (2006), Choosing a suitable analytical model for aerosol extinction spectra in the retrieval of UV/visible satellite occultation measurements, *J. Geophys. Res.*, *111*, D23203, doi:10.1029/2005JD006941.

1. Introduction

[2] Spaceborne monitoring of the Earth's atmosphere is performed using a number of optical methods, that differ in the wavelength range (UV, visible, infrared, radio waves) and target view (nadir, limb, and occulting Sun, stars or planets). Of all these methods, occultation measurements in the UV and visible have the advantage of delivering accurate constituent profile retrievals in terms of retrieval error and altitude resolution, although the amount of constituents that can be retrieved is rather limited (typically air density, O_3, NO_2, aerosol extinction). An additional advantage can be found in the fact that the associated retrieval algorithms are fairly straightforward and simple: there are no atmospheric source terms in the forward model, the measured signal is simply described by the transmittance of light through an absorbing and scattering medium, using the Beer-Lambert law. In this formulation, optical extinction by gases is expressed in a simple way. However, the situation is more complex for aerosols, since the particles in an aerosol population exhibit a wide range in sizes, and generally differ in chemical composition, morphology etc. The problem is usually handled by expressing the aerosol extinction spectrum as an analytical function of wavelength with a relatively small number of parameters that are to be retrieved. Still, the choice of analytical function and the actual number of parameters is far from obvious. In this paper, we will investigate the effect of the aerosol extinction model used on the retrieval quality of the background aerosols and the other species. To do this, we first generate a set of constituent profiles from which simulated transmittance measurements are calculated. Subsequently, we invert these measurements back to retrieved constituent profiles, using a variety of analytical aerosol extinction models. A comparison of "true" and retrieved constituent profiles leads to an estimate of the bias that is to be expected. The retrieval error and the chi-square statistics for the transmittance fit is also investigated.

2. Description of the Problem

[3] The actual optical extinction at a certain atmospheric location is expressed by the optical extinction coefficient. For gases, this coefficient equals the product of an extinction cross section C_{ext} with the quantity that is to be retrieved, the number density of the gas N:

$$\beta(\lambda) = C_{\text{ext}}(\lambda)N \tag{1}$$

[4] For aerosols (in general, for all particulate matter in the atmosphere, such as tropospheric cloud droplets or crystals and particles that constitute polar stratospheric or mesospheric clouds), the situation is more complex since we are dealing with populations of particles that are not

[1]Belgian Institute for Space Aeronomy, Brussels, Belgium.

0148-0227/06/2005JD006941

identical. If we assume a population consisting of particles that have the same morphology, chemical composition and state, and differ only in physical size, the extinction coefficient is expressed by the integral product of a cross section with a particle size distribution $\frac{dN(r)}{dr}$:

$$\beta(\lambda) = \int_0^\infty C_{ext}(\lambda, r) \frac{dN(r)}{dr} dr \quad (2)$$

In principle, after proper discretization of the integral [see, e.g., *King et al.*, 1978], it is possible to implement this expression in the retrieval scheme. There are three reasons why this is usually not done. First, the discretization of the size distribution introduces a large amount of new unknowns that are to be retrieved, which severely increases the computational cost. Second, the equation is ill posed: a large variety of different particle size distributions will lead, within measurement error, to the same aerosol extinction spectrum. The third reason is more subtle: atmospheric particle populations can exhibit variability in morphology, state and chemical composition, and it is a priori impossible to calculate the extinction cross section, with the consequence that equation (2) cannot be used directly. It is usually preferred to investigate retrieved aerosol extinction coefficients first, and make assumptions about the cross section in a later stage, during the retrieval of the size distribution.

[5] However, the problems associated with the first and second point are not necessarily solved when we retrieve aerosol extinction coefficients first. Present-day occultation spectra are measured with several hundreds or thousands of pixels. The retrieval of the aerosol extinction coefficient at all these wavelengths once again leads to a huge amount of unknowns and a severely ill-posed problem. The obvious way to avoid problems is to describe the aerosol extinction spectrum with an analytical function of wavelength, controlled by a small number of parameters. The question then rises: which analytical form should we implement, and how many parameters are necessary to capture the aerosol extinction behavior?

3. Simulation

[6] In order to find out what the effect is of a particular choice of aerosol extinction model on the retrieval of all species, we need retrievals that are obtained from simulated measurements, which in turn are calculated using known atmospheric constituent profiles. We therefore start with the construction of a set of altitude profiles for each constituent (gas densities and aerosol extinction). Using atmospheric weight functions and extinction cross sections, the associated transmittance can be calculated. We then artificially add "noise" to obtain a set of "measurements". The next step is to retrieve local gas density and aerosol extinction profiles, for each aerosol extinction model. After the retrieval, we are able to evaluate the retrieval noise (random and smoothing error), the bias, and the chi-square statistics of the transmittance.

3.1. Virtual Occultation Experiment

[7] Our instrument characteristics are based on the ones from the GOMOS (Global Ozone Monitoring by Occultation of Stars) instrument onboard the European Envisat satellite [*Bertaux et al.*, 1991, 2000; *Kyrölä et al.*, 2004; *European Space Agency*, 2001]. This is an arbitrary choice: the results and conclusions of this study are valid for all satellite occultation instruments equipped with a spectrometer that measures in the UV/Visible wavelength range.

[8] We assume a UV/Vis grating spectrometer having the GOMOS wavelength grid from 248 to 690 nm, with an average resolution of 0.31 nm. We take the instrument response to be perfect: it can be expressed by a Dirac delta function. Furthermore, we assume that the spectrometer performs instantaneous measurements (no readout delay) at a tangent altitude grid from 100 down to 10 km (the star is setting), with a distance of 1.8 km between two subsequent tangent altitudes. In reality, the grid spacing is irregular, and determined by the satellite orbit, velocity, the occultation angle with respect to the Earth's horizon, atmospheric refraction and the integration time of the spectrometer. We assume that the instrument observes the occultation of the star Sirius. The instrument adds thermal noise with a standard deviation that is constant for all wavelengths. A value was chosen in order to obtain a relative thermal noise level of 0.5% in the midvisible for the unattenuated Sirius spectrum.

3.2. Constituent Profiles

[9] Constructing a set of true gas concentration altitude profiles is a relatively straightforward task. For each gas, we start with a climatological altitude profile $\mathbf{N_c}$, taken from [*Anderson et al.*, 1986], and apply a transformation:

$$\mathbf{b_c} = \log(\mathbf{N_c}) \quad (3)$$

Working with $\mathbf{b_c}$ ensures that all gas concentrations will be positive. Also, as we will see, the algorithm that we use retrieves the quantity $\mathbf{b}$ instead of $\mathbf{N}$, once again to enforce positivity.

[10] A set of 100 profiles is generated by adding sinusoidal perturbations $\mathbf{s}^{(i)}$ to the profile:

$$\mathbf{b}^{(i)} = \mathbf{b_c} + \mathbf{s}^{(i)} \qquad i = 1 \cdots 100 \quad (4)$$

The perturbations $\mathbf{s}^{(i)}$ are calculated from amplitudes, phases and periods that are randomly drawn from normal distributions with a specified mean and variance. The statistics associated with the obtained set of 100 profiles for each gas are shown on Figure 1. All profiles have a grid spacing of 1 km, but the altitude range differs; air density profiles are specified from 10 to 80 km, ozone profiles from 10 to 110 km, and NO_2 from 10 to 60 km.

[11] When simulating background aerosol extinction profiles, it is not sufficient to add random sinusoidal perturbations, since the aerosol extinction coefficients at different wavelengths have to be physically consistent. It is better to perturb climatological values of a particle size distribution, and subsequently calculate the extinction coefficients using a Mie scattering code. Here, we assume a lognormal particle size distribution:

$$\frac{dN(r)}{dr} = \frac{N}{\sqrt{2\pi}\ln(s) r} \exp\left(-\frac{1}{2}\frac{\ln^2(r/r_m)}{\ln^2(s)}\right) \quad (5)$$

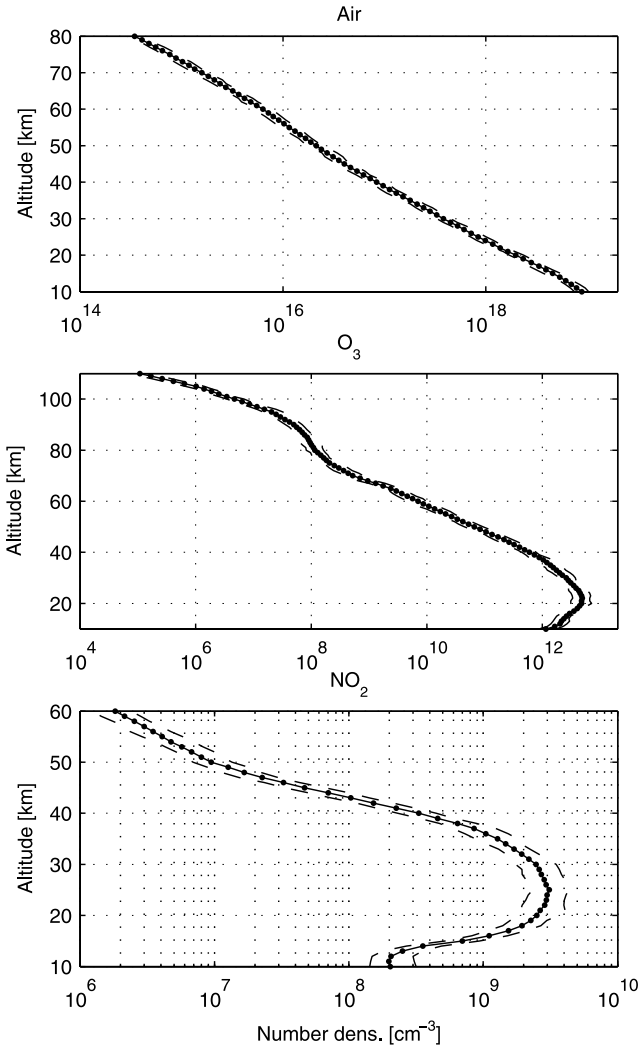

Figure 1. Statistics for the ensemble of 100 simulated gas concentration profiles. From top to bottom: air, O_3, and NO_2. Shown are the median (solid line with dots) and the 10th and 90th percentiles (dashed lines). Expressed in relative standard deviation, the ensemble has a variability (at all altitudes) of about 14% for air, 27% for O_3, and 27% for NO_2.

with N the total particle number density [cm^{-3}], r_m the median radius [μm] of the distribution, and s the geometrical standard deviation of the distribution (dimensionless). The values for N, r_m and $\sigma = \ln(s)$ that we use are based on the climatology of [*Bingen et al.*, 2004], and are representative for the year 2000, a period with low background stratospheric aerosol loading. Once again, a set of 100 altitude profiles for each parameter were generated by adding sinusoidal functions of altitude. Subsequently, the aerosol extinction at the spectrometer wavelengths can be calculated with equation (2). The extinction cross section C_{ext} is obtained from Mie theory [*Bohren and Huffman*, 1993], hereby assuming spherical particles composed of a sulfuric acid and water mixture, with a 75 percent mass fraction of H_2SO_4, and an associated refractive index of $1.43 + i0.00$. The obtained statistics for N, r_m, $\sigma = \ln(s)$ and $\beta_{aero}(500\ nm)$ are presented on Figure 2.

3.3. Simulated Transmittance

[12] Let us define the total atmospheric state vector $\mathbf{x_{tot}}$ as a vector containing all the quantities that have to be retrieved: the number densities of all gases, and the aerosol extinction coefficients, at all altitudes. The light intensity on the detector at tangent altitude h and wavelength λ is then theoretically expressed by the (discretized) Beer-Lambert law:

$$I(h,\lambda) = I_0(\lambda)\exp\left(-\mathbf{k}_{h,\lambda}^{T}\mathbf{x_{tot}}\right) \tag{6}$$

where $I_0(\lambda)$ is the unattenuated star spectrum (we chose Sirius as light source), and $\mathbf{k}_{h,\lambda}$ a vector containing the product of atmospheric contribution functions (the path lengths of the light ray in the individual atmospheric layers) with extinction cross sections (for gases) or aerosol model parameters. The ''measured'' light intensity can be simulated by adding Poisson shot noise and thermal noise:

$$I_{meas}(h,\lambda) = I(h,\lambda) + \epsilon_p + \epsilon_t \tag{7}$$

with $\sigma_p = \sqrt{I}$. Finally, we obtain the transmittance:

$$T(h,\lambda) = \frac{I_{meas}(h,\lambda)}{I_0(h,\lambda)} \tag{8}$$

[13] Using the set of 100 simulated constituent profiles, a set of 100 occultation measurements can be obtained in this way. The procedure is illustrated by Figure 3, where we show the unattenuated Sirius spectrum together with a

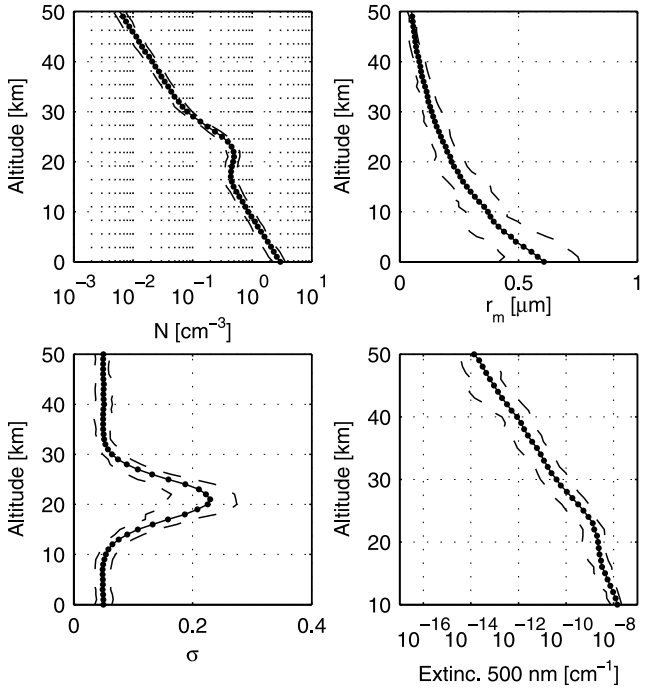

Figure 2. Statistics for the aerosol simulations: median (solid lines with dots) and 10th and 90th percentiles (dashed lines). Shown are (top left) total number density N, (top right) median radius r_m, (bottom left) distribution width σ, and (bottom right) simulated aerosol extinction at 500 nm.

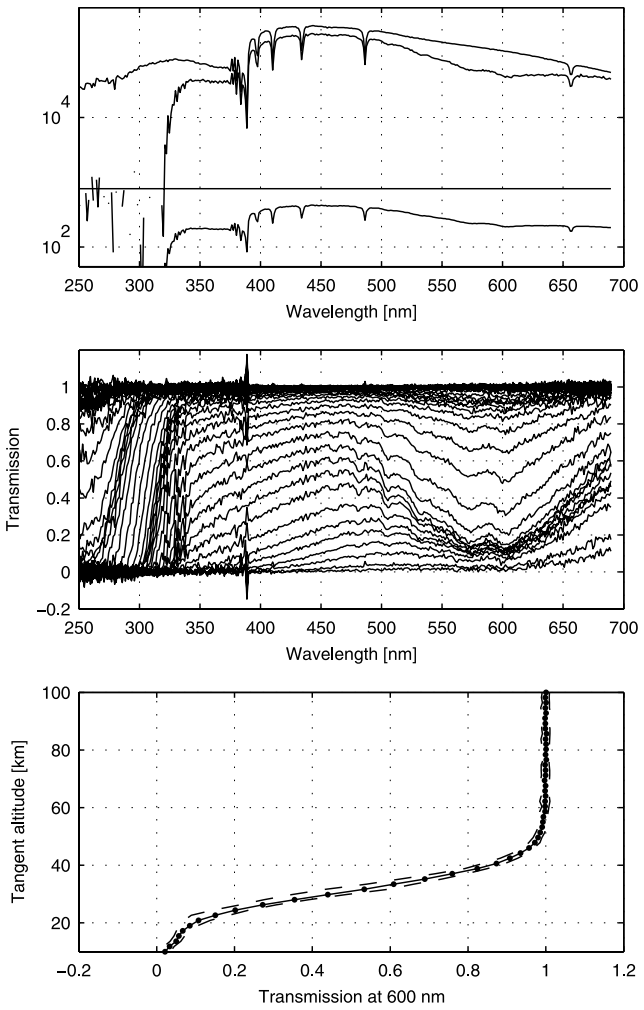

Figure 3. (top) From top to bottom, the unattenuated Sirius spectrum, a simulated signal at a tangent altitude of 29.5 km, the thermal noise, and the Poisson shot noise. (middle) One simulated transmittance realization. The curves represent spectra at subsequent tangent altitudes. (bottom) Median (solid line with dots) and 10th and 90th percentiles (dashed line) of all 100 simulated transmittances at 600 nm.

simulated signal at a tangent altitude of h = 29.5 km, and typical transmittance results.

4. Retrieval

4.1. Algorithm

[14] In a previously published paper [*Vanhellemont et al.*, 2004] we investigated the possibility of a global one-step retrieval of constituent profiles from a star occultation measurement. In such a retrieval scheme, all measured transmittances at all wavelengths and tangent altitudes are simultaneously inverted to all constituent profiles at all altitudes. Using such a method, no model approximations (neglection of chromatic refraction, effective extinction cross sections) have to be made, and all interdependences between all species at all altitudes are present in the model. The only disadvantage of such an approach lies in the fact that the full forward model matrix is too large to handle. *Vanhellemont et al.* [2004] dealt with this problem by using a retrieval method that is based on the singular value decomposition. Here we will use another approach that is conceptually more simple and computationally faster.

[15] Our principle goal is to retrieve an estimate of the atmospheric state vector $\mathbf{x_{tot}}$. However, to ensure positivity for all gas densities and aerosol extinction coefficients, we will retrieve its logarithm, $\mathbf{b_{tot}}$. We start with an a priori estimate of the full atmospheric state, $\mathbf{b_a}$ and $\mathbf{S_a}$. In our specific case, we take the a priori estimate to be the mean and covariance of the set of 100 simulated constituent profiles. If we denote the measured transmittance spectrum at the upper tangent altitude as $\mathbf{T_1}$, and the associated measurement error covariance matrix as $\mathbf{S_\epsilon 1}$, a first inversion is achieved by minimizing the cost function:

$$M_1 = \left[\mathbf{T_1} - \mathbf{T_{1,model}}(\mathbf{b})\right]^{\mathrm{T}} \mathbf{S_{\epsilon 1}}^{-1} \left[\mathbf{T_1} - \mathbf{T_{1,model}}(\mathbf{b})\right] + [\mathbf{b} - \mathbf{b_a}]^{\mathrm{T}} \mathbf{S_a}^{-1} [\mathbf{b} - \mathbf{b_a}] \quad (9)$$

Estimation by the minimization of such a merit function that is composed of a chi-square term and an a priori term is referred to as "optimal estimation", and the associated theory is given by *Rodgers* [2000]. The actual minimization is carried out with the Levenberg-Marquardt algorithm [*Rodgers*, 2000; *Press et al.*, 1992]. After convergence of the iterations, the solution $\mathbf{b_1}$ is obtained, while the solution covariance matrix $\mathbf{S_1}$ is obtained from the Jacobian of the objective function. The solution estimate $\mathbf{b_1}$ and $\mathbf{S_1}$ serves as the a priori for the inversion of the transmittance spectrum at the second tangent altitude. The cost function is expressed as

$$M_2 = \left[\mathbf{T_2} - \mathbf{T_{2,model}}(\mathbf{b})\right]^{\mathrm{T}} \mathbf{S_{\epsilon 2}}^{-1} \left[\mathbf{T_2} - \mathbf{T_{2,model}}(\mathbf{b})\right] + [\mathbf{b} - \mathbf{b_1}]^{\mathrm{T}} \mathbf{S_1}^{-1} [\mathbf{b} - \mathbf{b_1}] \quad (10)$$

A solution $\mathbf{b_2}$ and $\mathbf{S_2}$ is obtained, which will be used as an priori estimate for the inversion of the spectrum at the third tangent altitude. The procedure can be repeated until all n measured spectra are inverted. Using the final solution $\mathbf{b_{sol}} = \mathbf{b_n}$ and $\mathbf{S_{sol}} = \mathbf{S_n}$, the transmittance fit is calculated and the chi-square is evaluated at every tangent altitude separately.

[16] Mathematically, the solution $\mathbf{b_{sol}}$ and $\mathbf{S_{sol}}$ is equal to the solution of the full problem. The sequential steps are only necessary to make the calculations possible in practice, that is, using a realistic amount of computer memory within a reasonable execution time. Notice also that the method differs fundamentally from the well-known onion peeling procedure [*Rodgers*, 2000]: the entire state vector for all constituents and altitudes is updated for each tangent altitude, while in onion peeling only a local solution at the specified tangent altitude is obtained.

4.2. Models for Aerosol Extinction

[17] In general, aerosol extinction spectra in the UV and visible wavelength range vary smoothly with wavelength, due to the integral product of the particle extinction cross section with broad particle size distributions (equation (2)). This is why smooth analytical functions (such as low-degree polynomials) can be used to model these spectra. Table 1 lists the aerosol models that are used in the retrievals,

Table 1. Aerosol Extinction Models Used in the Retrievals

	Model	Retrieval Wavelengths, nm
M1	$\beta(\lambda) = 0$	-
M2	$\beta(\lambda) = c_0$	500
M3	$\beta(\lambda) = c_1/\lambda$	500
M4	$\beta(\lambda) = c_0 + c_1/\lambda$	(400, 500)
M5	$\beta(\lambda) = c_0 + c_1\ \lambda$	(400, 500)
M6	$\beta(\lambda) = c_0 + c_1\ \lambda + c_2\ \lambda^2$	(400, 500, 600)
M7	$\beta(\lambda) = c_0 + c_1\ \lambda + c_2\ \lambda^2 + c_3\ \lambda^3$	(300, 400, 500, 600)

together with the actual implementation (models, parametrized by extinction coefficients at a number of wavelengths), and the wavelengths where the actual aerosol extinction is retrieved. The following models were used. First, no aerosols are retrieved (model 1), just to check whether an aerosol retrieval is necessary in the first place. Model 2 is a simple constant function, independent of wavelength. Model 3 is an inverse wavelength law [see, e.g., *Vanhellemont et al.*, 2005], actually a special case of the Angstrom law $\beta_{\text{aero}} = A\lambda^{-\alpha}$ that is frequently used to model background stratospheric aerosols. Model 4 extends model 3 by the addition of a constant offset. Model 5 to 7 are functions with increasing complexity: a first, second and third-degree polynomial of wavelength. Especially the two last models have a special advantage: they can exhibit a maximum in the visible, a feature that is observed when larger (e.g., posteruptive) particles are present. Polynomials have already been explored in the past by teams associated with satellite instruments such as POAM III [*Lumpe et al.*, 2002] and SAGE III [*Brogniez et al.*, 2002], and balloon instruments such as AMON and SALOMON [*Berthet et al.*, 2002]. More information on aerosol extinction spectra can be found in the literature, for background [see, e.g., *Stevermer et al.*, 2000] as well as volcanic conditions [*Russell et al.*, 1996].

5. Results

[18] The inversion of the set of 100 simulated occultations with 7 different aerosol extinction models leads to 700 retrievals of the total state vector $\mathbf{b_{sol}}$ and covariance matrix $\mathbf{S_{sol}}$. After each retrieval, the results are transformed back to the state vector containing gas number densities and aerosol extinction coefficients:

$$\mathbf{x_{sol}} = \exp(\mathbf{b_{sol}}) \qquad \mathbf{S_{x,sol}} = \mathbf{X}\mathbf{S_{sol}}\mathbf{X}^{\mathrm{T}} \tag{11}$$

with $\mathbf{X}$ a matrix containing the vector $\mathbf{x_{sol}}$ on its diagonal, and zeros elsewhere. The 700 retrievals can now be used to derive conclusions on the effect of the chosen aerosol model on the retrieval quality.

5.1. Retrieval Error

[19] Retrieval error is obtained from the square root of the diagonal of $\mathbf{S_{x,sol}}$. The median retrieval errors for air, O_3, NO_2 and aerosol extinction at 500 nm are presented by Figure 4. For the gases, the observations can be summarized as follows: the more aerosol model parameters, the larger

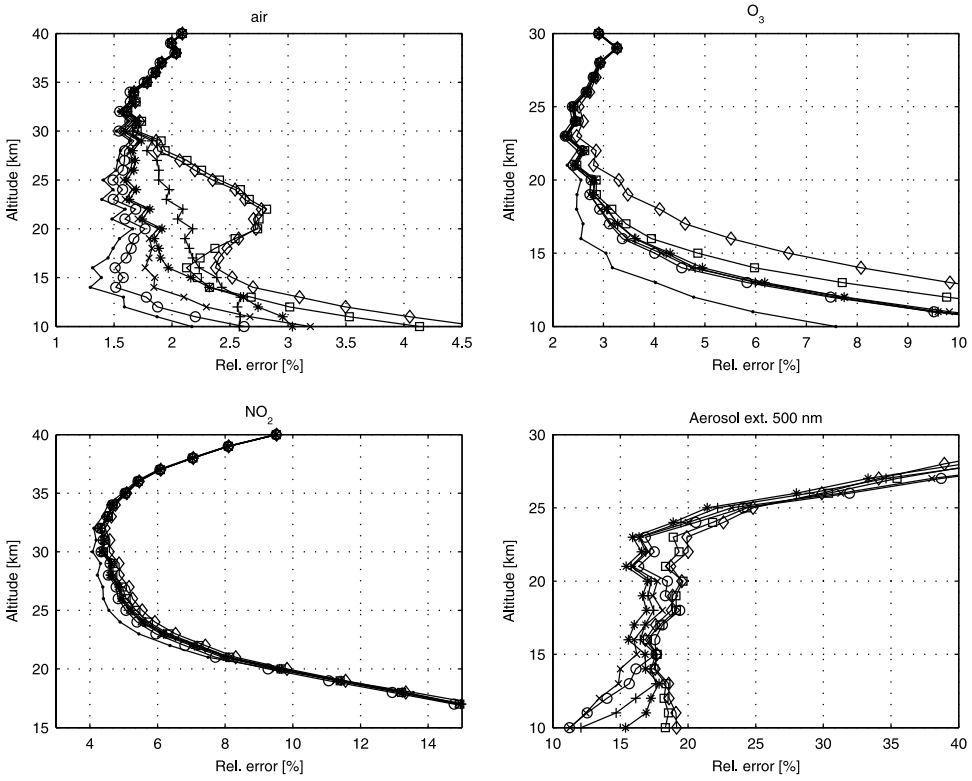

Figure 4. Relative median retrieval error for each constituent, evaluated for the different aerosol models: M1 (solid circles), M2 (open circles), M3 (crosses), M4 (pluses), M5 (asterisks), M6 (squares), and M7 (diamonds).

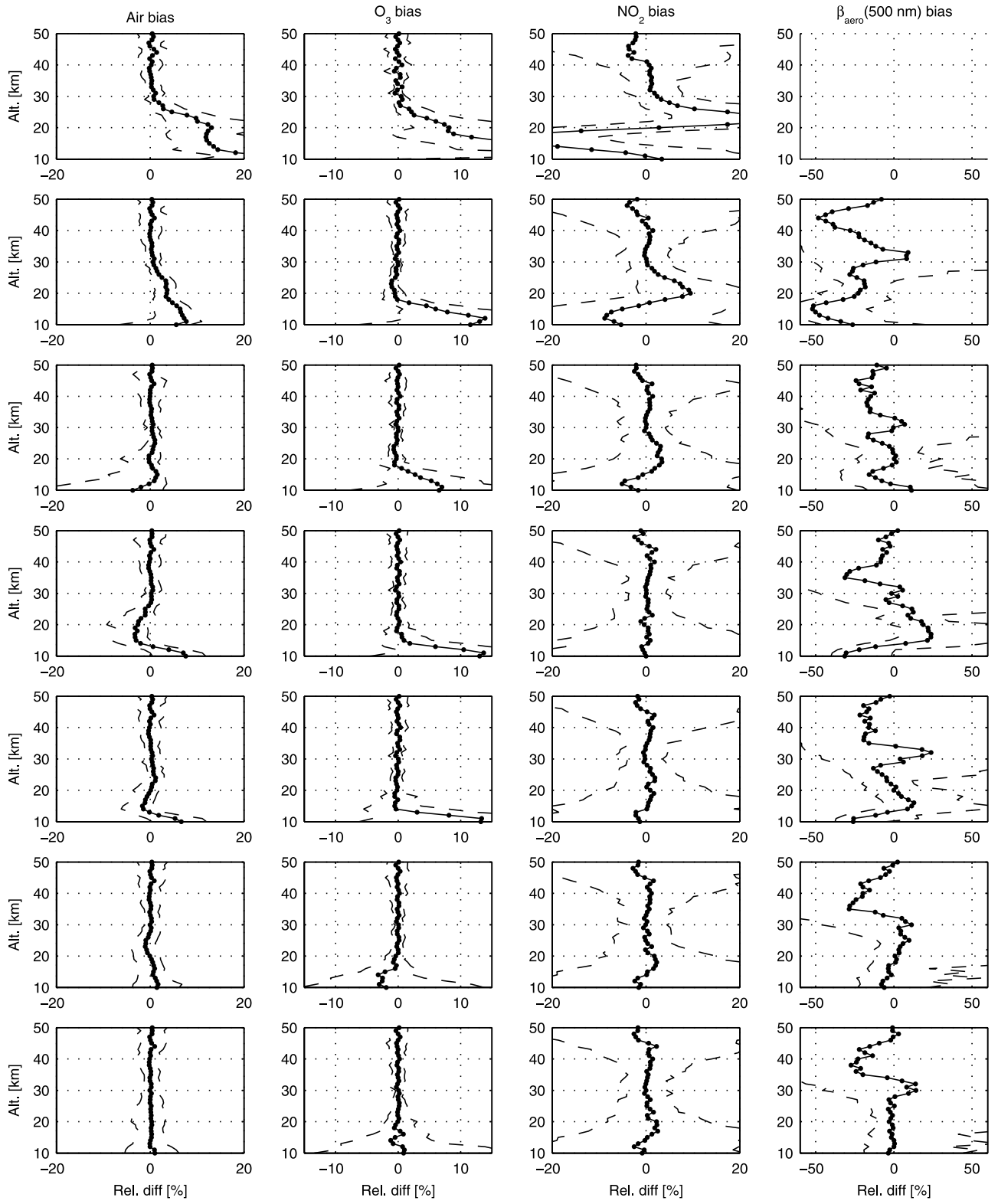

Figure 5. Median retrieval bias for all constituents (left to right), using the different aerosol models M1 to M7 (top to bottom). Also shown are the 10th and 90th percentile (dashed lines).

the retrieval error. However, the effect is minimal: for air retrievals, it is a matter of a few percent, for NO_2 it is negligible. The conclusion is different for ozone retrievals below 22 km, where we observe significantly larger retrieval errors (up to 5%) when using more complex aerosol models. For aerosols, clear conclusions are more difficult to draw: above 25 km, we observe a retrieval error decrease with increasing number of aerosol parameters, while the reverse is true at lower altitudes. However, the effect is once again far from dramatic.

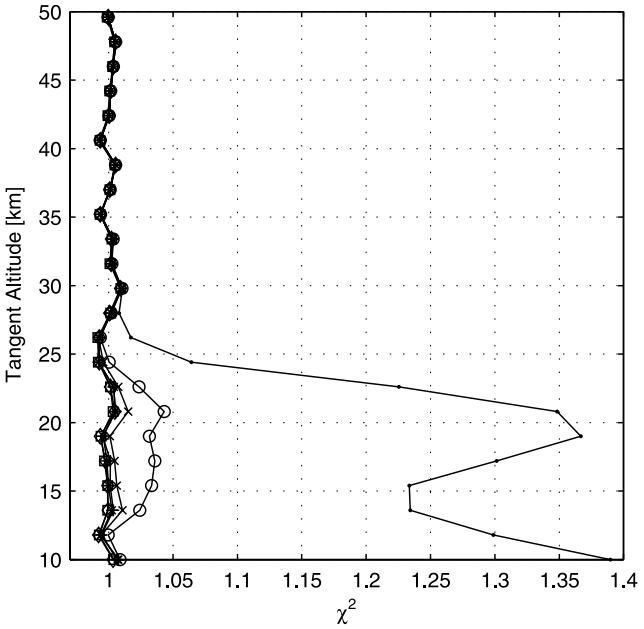

Figure 6. Normalized chi-square at every tangent altitude for the different aerosol models: M1 (solid circles), M2 (open circles), M3 (crosses), M4 (pluses), M5 (asterisks), M6 (squares), and M7 (diamonds).

5.2. Bias

[20] The systematic error that is caused by a wrong aerosol extinction model specification can be evaluated by comparing the retrievals with the true state. The median relative bias of the ith component of the retrieval $\mathbf{x_{sol}}$ is calculated as

$$p_i = \text{median}\left(100\frac{x_{\text{sol},i} - x_{\text{true},i}}{x_{\text{true},i}}\right) \tag{12}$$

[21] The median bias for all constituents and aerosol extinction models is shown in Figure 5, together with the 10th and 90th percentiles. As expected, all constituents show a decreasing bias for an increasing number of aerosol model parameters. When no aerosol model is implemented, all constituent retrievals exhibit a very strong bias. This is an important result; even with the simulated low stratospheric aerosol loading, a significant aerosol extinction signature is present in the measured spectra, and it has to be taken into account during the retrieval stage.

[22] Generally, we can conclude that air retrievals are not influenced by the choice of aerosol model above an altitude of 30 km. At lower altitudes, bias can only be neglected when a quadratic or third degree aerosol model is implemented.

[23] For ozone, the use of a simple constant aerosol model already improves the retrieval considerably, with essentially bias-free results above 20 km. Below this altitude, ozone retrievals usually contain quite large biases. Only with the implementation of a second or third-degree aerosol polynomial the bias is acceptably small.

[24] The NO_2 retrievals show a quite large bias below 30 km, that gradually decreases when the aerosol model used is more complex. The bias is already acceptably small when a relative simple aerosol model with two parameters (a linear polynomial) is used, and the bias does not seem to decrease considerably with more complex aerosol models.

[25] Investigation of the 500 nm aerosol extinction retrievals below 30 km shows that the bias keeps decreasing when more complex aerosol models are implemented. However, an acceptable low bias is obtained when using a second or third-degree polynomial. At altitudes above 30 km, the results are more difficult to interpret due to the low retrieval accuracy, which is caused by the low aerosol abundance.

5.3. Chi-Square

[26] The normalized chi-square statistics for the transmittance at tangent altitude i is obtained as follows:

$$\left[\left(\mathbf{T_i} - \mathbf{T_{i,model}}(\mathbf{b})\right)^{\mathrm{T}}\mathbf{S_{ei}}^{-1}\left(\mathbf{T_i} - \mathbf{T_{i,model}}(\mathbf{b})\right)\right]/n \tag{13}$$

with n the number of elements in the vector $\mathbf{T_i}$, or the number of spectral pixels. The results are shown on Figure 6. The conclusions is clear: above 30 km, no effect can be seen, and at lower altitudes the χ^2 decreases with increasing number of aerosol model parameters. Two parameters or more are necessary to obtain a good fit.

5.4. Aerosol Spectral Behavior

[27] If one wants to derive particle size distributions from aerosol extinction retrievals, it is important to use an

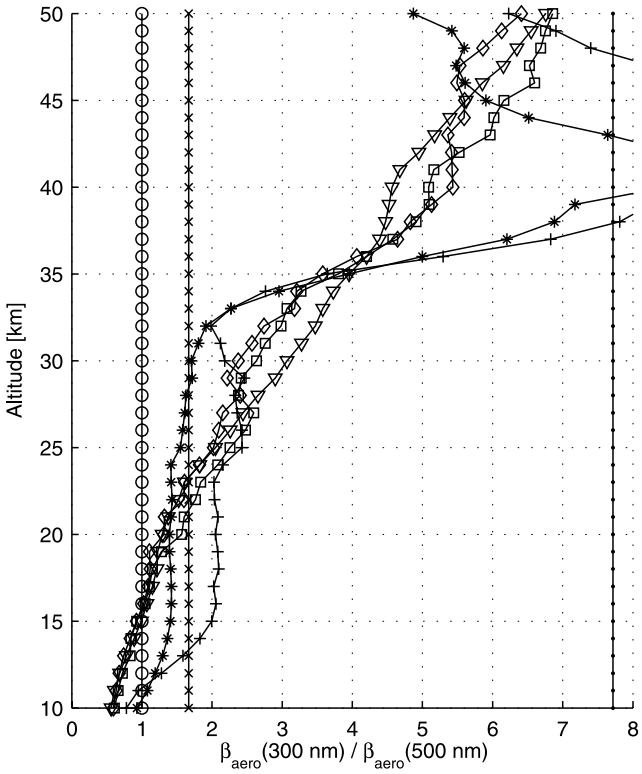

Figure 7. Ratio of aerosol extinction at 300 and 500 nm: median values for the set of 100 retrievals, using different aerosol models: M2 (the large particle limit; circles), M3 (crosses), M4 (pluses), M5 (asterisks), M6 (squares), and M7 (diamonds). Also shown are the small particle limit (solid circles) and the true values (inverted triangles).

appropriate aerosol extinction model that is able to capture the true aerosol spectrum. The ratio of aerosol extinction coefficients at two wavelengths is one way to quantify the spectral behavior. Figure 7 shows the ratio of β_{aero} at 300 and 500 nm. From Mie theory, we know that the small particle limit results in the Rayleigh scattering law, $\beta_{aero} = A\lambda^{-4}$, giving a ratio of $(500/300)^4 = 7.72$. In the large particle limit on the other hand, the spectrum is constant, with a ratio equal to 1. In between these two cases, a wide range of ratios are possible. Figure 7 clearly shows that only a second or third-degree polynomial is able to capture the aerosol spectral behavior at all altitudes. We can therefore conclude that for aerosol studies the implementation of at least a second-degree polynomial is imperative.

6. Conclusion

[28] Retrieval algorithms that derive constituent altitude profiles from satellite occultation measurements in the UV and visible wavelength range deal with an aerosol extinction contribution by modeling the extinction spectrum by a relatively simple analytical function. The actual choice of model is far from straightforward, but can be guided by the fact that retrieval error and retrieval bias counterbalance each other: the more parameters in the aerosol model, the larger the retrieval error, and the smaller the bias. It is therefore desirable to keep the number of aerosol parameters as small as possible, while retaining enough parameters to keep the bias acceptably low. The problem can be expressed in another way, guided by the functionality of the retrievals. If the goal of the retrieval is to build climatologies, by averaging retrieval ensembles, it is preferred to have results that exhibit a bias that is as small as possible. In this case, a more complex aerosol model is advantageous. On the other hand, if we want to make use of individual retrievals (say, for validation of gas concentrations and aerosol extinction coefficients with other experiments), it is better to use simpler aerosol models, since the associated retrieval error is low. The results in this paper represent an optimal case, because Sirius, the brightest star, was chosen as the light source. The importance of the retrieval error will most likely be larger when using weaker stars. Having said this, we can draw the following conclusions. Although retrieval error gets larger when complex aerosol models are used, the actual increase is usually quite small, except for ozone below 20 km. Bias, induced by a wrongly specified aerosol extinction model, is negligible above 30 km for all species, but becomes increasingly more important at lower altitudes. In this region, more complex aerosol models have to be used to avoid bias. As a good all-round rule, we can say that at least a second or third degree polynomial has to be used.

[29] **Acknowledgments.** This work was financially supported with the Prodex 7 contract "SADE" and a grant (MO/35/009) from the Federal Office for Scientific, Technical and Cultural Affairs (OSTC) of the Belgian government.

References

Anderson, G., S. Clough, F. Kneizys, J. Chetwynd, and E. Shettle (1986), AFGL atmospheric constituent profiles (0–120 km), *Tech. Rep. AFGL-TR-86-0110*, Air Force Geophys. Lab., Hanscom Air Force Base, Bedford, Mass.

Bertaux, J., G. Megie, T. Widemann, E. Chassefiere, R. Pellinen, E. Kyrölä, S. Korpela, and P. Simon (1991), Monitoring of ozone trend by stellar occultations: The GOMOS instrument, *Adv. Space Res.*, *11*(3), 3237–3242.

Bertaux, J., E. Kyrölä, and T. Wehr (2000), Stellar occultation technique for atmospheric ozone monitoring: GOMOS on Envisat, *Earth Obs. Q.*, (67), 17–20.

Berthet, G., J.-B. Renard, C. Brogniez, C. Robert, M. Chartier, and M. Pirre (2002), Optical and physical properties of stratospheric aerosols from balloon measurements in the visible and near-infrared domains. I. Analysis of aerosol extinction spectra from the AMON and SALOMON balloonborne spectrometers, *Appl. Opt.*, *41*(36), 7522–7539.

Bingen, C., D. Fussen, and F. Vanhellemont (2004), A global climatology of stratospheric aerosol size distribution parameters derived from SAGE II data over the period 1984–2000: 2. Reference data, *J. Geophys. Res.*, D06202, doi:10.1029/2003JD003511.

Bohren, C., and D. Huffman (1993), *Absorption and Scattering of Light by Small Particles*, John Wiley, Hoboken, N. J.

Brogniez, C., A. Bazureau, J. Lenoble, and W. P. Chu (2002), Stratospheric Aerosol and Gas Experiment (SAGE) III measurements: A study on the retrieval of ozone, nitrogen dioxide, and aerosol extinction coefficients, *J. Geophys. Res.*, *107*(D24), 4758, doi:10.1029/2001JD001576.

European Space Agency (2001), Envisat–GOMOS—An instrument for global atmosphere ozone monitoring, *Eur. Space Agency Spec. Publ., ESA SP-1244*, 109 pp.

King, M., D. Byrne, B. Herman, and J. Reagan (1978), Aerosol size distributions obtained by inversion of spectral optical depth measurements, *J. Atmos. Sci.*, *35*, 2153–2167.

Kyrölä, E., et al. (2004), GOMOS on Envisat—An overview, *Adv. Space Res.*, *33*, 1020–1028.

Lumpe, J. D., R. M. Bevilacqua, K. W. Hoppel, and C. E. Randall (2002), POAM III retrieval algorithm and error analysis, *J. Geophys. Res.*, *107*(D21), 4575, doi:10.1029/2002JD002137.

Press, W., S. Teukolsky, W. Vetterling, and B. Flannery (1992), *Numerical Recipes in FORTRAN: The Art of Scientific Computing*, 2nd ed., Cambridge Univ. Press, New York.

Rodgers, C. (2000), *Inverse Methods for Atmospheric Sounding: Theory and Practice*, World Sci., Hackensack, N. J.

Russell, P., et al. (1996), Global to microscale evolution of the Pinatubo volcanic aerosol derived from diverse measurements and analyses, *J. Geophys. Res.*, *101*, 18,745–18,763.

Stevermer, A. J., I. V. Petropavlovskikh, J. M. Rosen, and J. J. DeLuisi (2000), Development of a global stratospheric aerosol climatology: Optical properties and applications for UV, *J. Geophys. Res.*, *105*, 22,763–22,776.

Vanhellemont, F., D. Fussen, and C. Bingen (2004), Global one-step inversion of satellite occultation measurements: A practical method, *J. Geophys. Res.*, *109*, D09306, doi:10.1029/2003JD004168.

Vanhellemont, F., et al. (2005), A 2003 stratospheric aerosol extinction and PSC climatology from GOMOS on Envisat, *Atmos. Chem. Phys.*, *5*, 2413–2417.

C. Bingen, J. Dodion, D. Fussen, N. Mateshvili, and F. Vanhellemont, Belgian Institute for Space Aeronomy, Ringlaan 3, B-1180, Brussels, Belgium. (filip.vanhellemont@bira-iasb.oma.be)